Disappearance of the last tropical glaciers in the Western Pacific Warm Pool (Papua, Indonesia) appears imminent

Donaldi S. Permana[a,b,c,1], Lonnie G. Thompson[b,c,1], Ellen Mosley-Thompson[b,d], Mary E. Davis[b], Ping-Nan Lin[b], Julien P. Nicolas[b], John F. Bolzan[b], Broxton W. Bird[e], Vladimir N. Mikhalenko[f], Paolo Gabrielli[b,c], Victor Zagorodnov[b], Keith R. Mountain[g], Ulrich Schotterer[h], Wido Hanggoro[a], Muhammad N. Habibie[a], Yohanes Kaize[i], Dodo Gunawan[a], Gesang Setyadi[i], Raden D. Susanto[j,k], Alfonso Fernández[l], and Bryan G. Mark[b,d]

[a]Center for Research and Development, Agency for Meteorology Climatology and Geophysics (Badan Meteorologi, Klimatologi, dan Geofisika), Jakarta 10720, Indonesia; [b]Byrd Polar and Climate Research Center, The Ohio State University, Columbus, OH 43210; [c]School of Earth Sciences, The Ohio State University, Columbus, OH 43210; [d]Department of Geography, The Ohio State University, Columbus, OH 43210; [e]Department of Earth Sciences, Indiana University–Purdue University, Indianapolis, IN 46202; [f]Institute of Geography, Russian Academy of Sciences, Moscow 119017, Russia; [g]Department of Geography and Geosciences, University of Louisville, Louisville, KY 40292; [h]Climate and Environmental Physics Group, University of Bern, 3012 Bern, Switzerland; [i]Environmental Department, PT Freeport Indonesia, Timika, Papua 99971, Indonesia; [j]Department of Atmospheric and Oceanic Sciences, University of Maryland, College Park, MD 20742; [k]Faculty of Earth Science and Technology, Bandung Institute of Technology, Bandung 40132, Indonesia; and [l]Departamento de Geografía, Universidad de Concepción, Concepción 4070386, Chile

Edited by Michael L. Bender, Princeton University, Princeton, NJ, and approved November 5, 2019 (received for review December 27, 2018)

The glaciers near Puncak Jaya in Papua, Indonesia, the highest peak between the Himalayas and the Andes, are the last remaining tropical glaciers in the West Pacific Warm Pool (WPWP). Here, we report the recent, rapid retreat of the glaciers near Puncak Jaya by quantifying the loss of ice coverage and reduction of ice thickness over the last 8 y. Photographs and measurements of a 30-m accumulation stake anchored to bedrock on the summit of one of these glaciers document a rapid pace in the loss of ice cover and a ∼5.4-fold increase in the thinning rate, which was augmented by the strong 2015–2016 El Niño. At the current rate of ice loss, these glaciers will likely disappear within the next decade. To further understand the mechanisms driving the observed retreat of these glaciers, 2 ∼32-m-long ice cores to bedrock recovered in mid-2010 are used to reconstruct the tropical Pacific climate variability over approximately the past half-century on a quasi-interannual timescale. The ice core oxygen isotopic ratios show a significant positive linear trend since 1964 CE (0.018 ± 0.008‰ per year; $P < 0.03$) and also suggest that the glaciers' retreat is augmented by El Niño–Southern Oscillation processes, such as convection and warming of the atmosphere and sea surface. These Papua glaciers provide the only tropical records of ice core-derived climate variability for the WPWP.

glacier retreat | tropical ice cores | Papua Indonesia | climate change | ENSO

Tropical glaciers are highly sensitive indicators and recorders of climate changes (1). Unfortunately, most tropical glaciers are currently in retreat (2–7) due primarily to recent anthropogenic atmospheric warming, although strong El Niños play an intermittent role in many regions by increasing air temperature and decreasing precipitation (8–10). The warmest global sea surface and upper level atmospheric temperatures occur in the Western Pacific Warm Pool (WPWP) where the associated energy drives intense and deep convective precipitation (11). Here, we present the recent, rapid retreat of the last tropical glaciers in the WPWP by quantifying the loss of ice coverage and reduction of ice thickness over the last 8 y. Total ice loss was assessed by implementing a glacier mass balance model and future regional climate model projections for the region under different climate scenarios. We also present an ice core-derived tropical Pacific climate reconstruction from these glaciers on an interannual [El Niño–Southern Oscillation (ENSO)] timescale from 1964 to ∼2010 CE in order to help understand the mechanisms driving their observed retreat.

Study Site

The glaciers near Puncak Jaya in Papua, Indonesia (4.083°S; 137.167°E; 4,884 m above sea level), which prior to 2002 was also known as Irian Jaya, are located within an east–west-oriented mountain range on the western half of the island of New Guinea (Fig. 1*A*). These glaciers are the last remaining tropical glaciers in the WPWP, the heat engine for Earth's climate system, and sit near the highest peak (Carstensz Pyramid) between the Himalayas and the Andes. At lower elevations, the island is

Significance

The glaciers near Puncak Jaya, Papua, Indonesia, the last tropical glaciers in the Western Pacific Warm Pool, have recently undergone a rapid pace of loss of ice cover and a 5.4-fold increase in the rate of thinning, augmented by the strong 2015–2016 El Niño. Ice cores recovered in 2010 record approximately the past half-century of tropical Pacific climate variability and reveal the effects of El Niño–Southern Oscillation (ENSO). It appears that the regional warming has passed a threshold such that the next very strong ENSO event, which typically exacerbates the rising freezing levels and associated feedbacks such as reduced snow cover, could lead to the demise of the only remaining tropical glaciers between the Himalayas and the Andes.

Author contributions: L.G.T., E.M.-T., and R.D.S. designed research; D.S.P., L.G.T., E.M.-T., M.E.D., P.-N.L., B.W.B., V.N.M., P.G., V.Z., K.R.M., W.H., M.N.H., Y.K., D.G., G.S., and R.D.S. performed research; D.S.P., L.G.T., M.E.D., P.-N.L., J.P.N., J.F.B., U.S., A.F., and B.G.M. analyzed data; D.S.P., L.G.T., E.M.-T., and M.E.D. wrote the paper; D.S.P., L.G.T., V.N.M., P.G., V.Z., K.R.M., W.H., Y.K., D.G., G.S., and R.D.S. supported the ice core drilling project and collected ice core samples; D.S.P., L.G.T., K.R.M., W.H., M.N.H., Y.K., and G.S. measured the stake accumulation; M.E.D., and P.-N.L. conducted the ice core stable isotope, dust, and chemical analyses; and U.S. conducted the ice core tritium analysis.

The authors declare no competing interest.

This article is a PNAS Direct Submission.

Data deposition: The data reported in this paper have been archived at the National Center for Environmental Information (NCEI) National Oceanic and Atmospheric Administration (NOAA) World Data Center for Paleoclimatology: https://www.ncdc.noaa.gov/data-access/paleoclimatology-data/datasets/ice-core; https://www.ncdc.noaa.gov/paleo/study/24351.

[1]To whom correspondence may be addressed. Email: donaldi.permana@bmkg.go.id or thompson.3@osu.edu.

This article contains supporting information online at https://www.pnas.org/lookup/suppl/doi:10.1073/pnas.1822037116/-/DCSupplemental.

First published December 9, 2019.

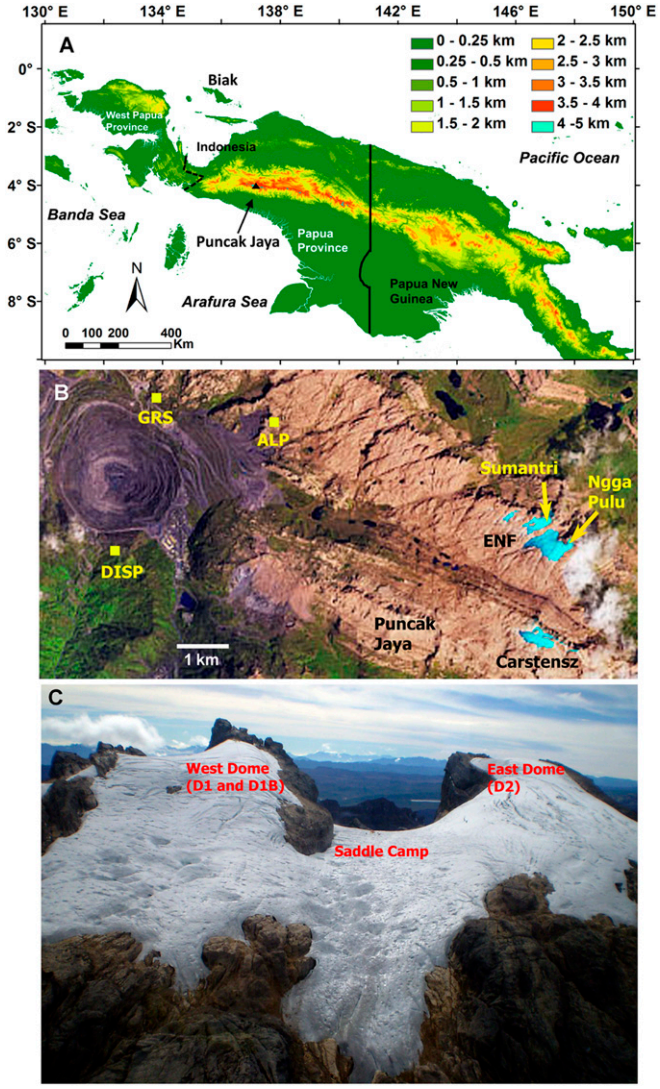

Fig. 1. Geographical and physical setting of the Papua ice fields. (*A*) Topography of New Guinea Island, showing the location of Puncak Jaya in Papua. (*B*) Papua glaciers and locations of stations with available instrumental records (DISP, GRS, and ALP) (background image: https://eoimages.gsfc.nasa.gov/images/imagerecords/91000/91716/puncak_oli_2017339_lrg.jpg). (*C*) Oblique aerial photo taken in June 2010 of the ENF, showing the locations of the drill sites on the west and east domes. The distance between the summits of the domes is about 600 m.

covered mainly by tropical lowland and montane rainforest. As one of Earth's wettest regions, many sites in Papua receive 2,500 to 4,500 mm of precipitation annually, with up to ∼12,500 mm falling on the southern slope of the central Maoke Mountains (12, 13). In general, Papua experiences wet conditions during austral summer (December to March) and relatively drier conditions, particularly on the southern part of the island, during austral winter (May to October). Interannual precipitation variability is strongly linked to ENSO, with El Niño events generally associated with dry conditions, enhanced dust, and increased biomass burning, with opposite conditions dominating during La Niña events (14). The stable oxygen ($\delta^{18}O$) and hydrogen (δD) isotopic ratios in precipitation on Papua are controlled by regional convective activity at daily to interannual timescales with higher $\delta^{18}O$ values (e.g., enriched in ^{18}O) during El Niño years (13).

Most mountain glaciers around the world are retreating (15), and for many sites atmospheric warming has been identified as the main factor affecting ice loss (16). Likewise, the glaciers near Puncak Jaya have been retreating since the end of the most recent neoglacial period ∼1850 CE (17). Total glacier area has decreased from ∼19 km^2 in ∼1850 (18, 19) to ∼1.8 km^2 in 2005 (20). An ice core drilling campaign was conducted in Papua in May to June 2010 during which 3 cores were recovered from the East Northwall Firn (ENF) (Fig. 1 *B* and *C*). Two ice cores, measuring 32.13 m (D1) and 31.25 m (D1B) in depth, were drilled to bedrock and extracted from the west dome (Sumantri Peak) and a third core (D2), measuring 26.19 m, was extracted from the east dome (Soekarno Peak/Ngga Pulu) (1, 17). At the same time, a flexible accumulation "stake" composed of 15, 2-m-long polyvinyl chloride (PVC) pipes linearly connected by rope was placed in the D1 borehole (4°03′ S; 137°11′ E) (Fig. 2*A* and *SI Appendix*, Fig. S1*A*).

Results and Discussion

Ice Thickness Reduction. Changes in ice thickness since June 2010 were determined by measuring the accumulation stake during subsequent visits to the drill site, which revealed progressive exposure of PVC sections due to surface ice loss (*SI Appendix*, Fig. S1 *B–D*). During the first site visit on November 3, 2015, 2 pipe segments and 1.49 m of rope were observed lying on the surface, indicating that the ice had thinned a total of ∼5 m at a rate of ∼1.05 m/y since 2010 (Fig. 2*A* and *SI Appendix*, Fig. S1*B*). During a monitoring visit on May 31, 2016, 4 pipe segments were exposed at the surface (Fig. 2*A* and *SI Appendix*, Fig. S1*C*), indicating an additional ice thinning of ∼4.26 m within just over 6 mo. This was likely due to the effects of the very strong 2015–2016 El Niño. The most recent measurement on November 23, 2016, revealed

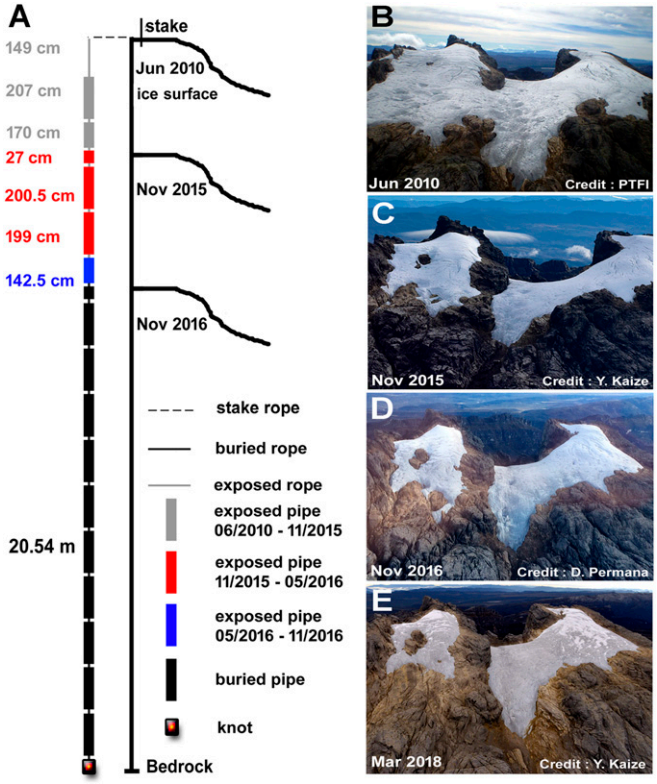

Fig. 2. Ice thinning and retreat of Papua glaciers. (*A*) Schematic of connected PVC pipes illustrating ice thickness changes on the ENF in June 2010, November 2015 (gray), May 2016 (red), and November 2016 (blue). Oblique aerial photographs of the ENF taken in (*B*) June 2010, (*C*) November 2015, (*D*) November 2016, and (*E*) March 2018 show the bifurcation of the ice mass.

an additional 1.43 m of ice thinning since May 2016, confirming that, although the annual rate of thinning had slowed, it remained 2.7 times greater than the average rate from 2010 to 2015 (Fig. 2*A* and *SI Appendix*, Fig. S1*D*). This thinning accompanied the progressive contraction of the glacier surface area resulting in the separation of the ENF into 2 ice masses (Fig. 2 *B*–*E*). These measurements illustrate the overall rapid rate of ice thinning as well as the particularly strong impact of the temperature increase and precipitation decrease associated with the 2015–2016 El Niño.

Ice Coverage Loss. The 2 remaining large glaciers near Puncak Jaya (Fig. 3*A*) experienced a dramatic loss of ice coverage from 2002 to 2018 that intensified during the 2015–2016 El Niño (Fig. 3 *B* and *C*). The new data from 2015, 2016, and 2018 are integrated with those from previous observations (17) to show that the total glacier area near Puncak Jaya has decreased linearly from ∼1850 to 2018 (Fig. 3*D*). From 2002 to 2015, the ice cover diminished by 1.45 km^2, equivalent to a loss rate of 0.11 km^2 per y. During the 2015–2016 El Niño, an additional 0.11 km^2 of ice cover was lost from 2015 to 2016. In March 2018, the ice cover was only 0.458 ± 0.036 km^2 or a loss of 0.09 km^2 since 2016. During the period from 2002 to 2018, the glacier retreated at a rapid but steady pace (Fig. 3*D*, *Inset*).

The closest available instrumental records of temperature and precipitation are located 50 to 450 m below the minimum glacierized elevation (Grasberg [GRS], Dispatch Tower [DISP], and Alpine [ALP] stations, Fig. 1*B*) and cover the period 1997–2016 (*SI Appendix*, Table S2). Although these records have a number of data gaps, they indicate a near-zero probability that average daily temperatures have fallen below the freezing point since 1997 (*SI Appendix*, Fig. S2). This assumption is supported by calculating freezing levels from the average temperature at the nearest station (ALP) using 2 realistic lapse rates, i.e., the mean lapse rate between GRS-DISP and GRS-ALP (4.6 °C/km) (*SI Appendix*, Fig. S3), and the environmental lapse rate (6.5 °C/km), to identify the remaining ice surface that lies above the freezing line. Coupling these freezing levels with 3 different hypsometric curves of the glacierized area indicate that between 0 and 10% of the remaining ice surface lies above the freezing line (*SI Appendix*, Fig. S4). Thus, even with steep lapse rates, this hypsometric distribution implies that prevailing temperatures are generally above freezing over the glaciers, which promotes glacier melting. Furthermore, accumulation during these warm conditions is restricted to a few hours during the night and only over the highest elevations where frozen precipitation covers a small fraction of the glacierized area (*SI Appendix*, Fig. S5).

Glacier Mass Balance Model and Shrinkage Projections. The rapid rate of area loss and dramatic ∼5.4-fold increase in the rate of thinning in 2015–2016 present a scenario of unstoppable glacier demise. Depending on the interannual variability of temperature and precipitation over the next few years, the remaining ice fields of Papua, Indonesia, are very likely to disappear during the next decade. To provide a quantitative basis for this scenario, a glacier mass balance model was implemented by combining the available instrumental climatic records and dynamical/statistical downscaling of future climate model projections for the region under different climate scenarios (*SI Appendix*, Figs. S6 and S7 and Tables S3 and S4). We performed simulations of glacier volumetric change for the period 2017–2030 using a spatially distributed mass balance model. The model computes the difference between ablation and accumulation at daily time steps and transforms that change into volume relative to initial volume. Surface area reported in the Randolph Glacier Inventory (RGI) (21) is utilized to compute an initial volume of 0.13 km^3 according to an area–volume scaling (22, 23). Ablation is calculated from daily positive temperatures while accumulation utilizes temperature thresholds to determine the amount of solid precipitation falling over the glacierized area.

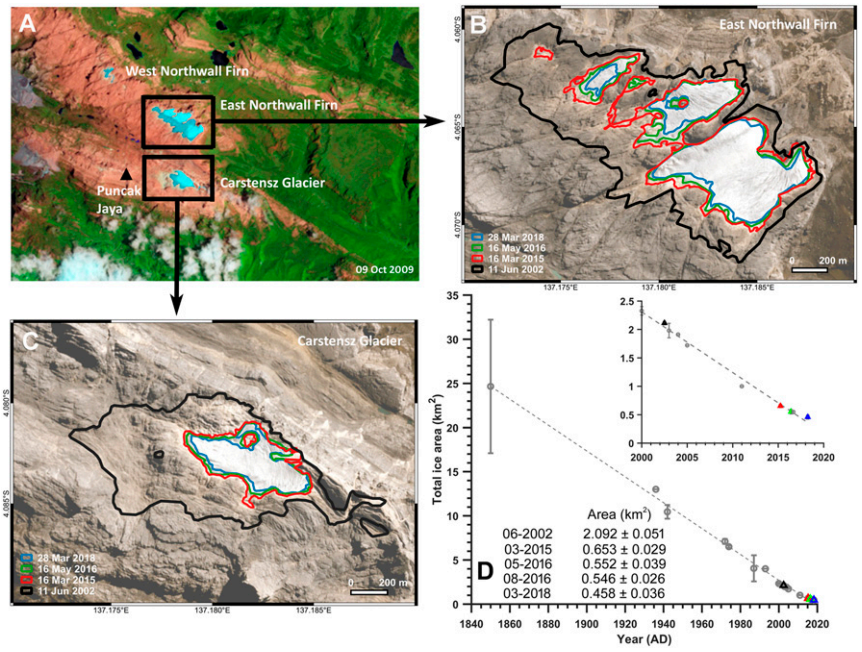

Fig. 3. Changes of total ice area and impact of the 2015–2016 El Niño on Papua glaciers. (*A*) Landsat-5 satellite image of the glaciated area on October 9, 2009. The ENF and the Carstensz Glacier are outlined in black boxes. (*B*) Planet's satellite image of ENF taken on May 16, 2016, showing outlines of ice extent on June 11, 2002 (as in ref. 6); March 16, 2015; May 16, 2016; and March 28, 2018. (*C*) Planet's satellite image of Carstensz Glacier taken on May 16, 2016, showing outlines of ice extent on same dates as in *B*. (*D*) The changes of total glacier area near Puncak Jaya from ∼1850 to 2018. The *Inset* highlights the ice area changes from 2002 to 2018. Color-coded triangles depict the coverage outlined in *B* and *C*; the gray circles and uncertainty bars are derived from other studies (17). Additional information on the satellite images in *B* and *C* are provided in *SI Appendix*, Table S1.

The model was evaluated and calibrated to reproduce the surface thinning based on the available stake measurements by using optimal combinations of lapse rates derived from the closest instrumental records of temperature and precipitation. Simulation of volumetric changes was driven by climate model projections over the Southeast Asia region (Southeast Asia Regional Climate Downscaling [SEACLID]/Coordinated Regional Climate Downscaling Experiment–Southeast Asia [CORDEX-SEA] project; http://www.ukm.edu.my/seaclid-cordex). The model predicts that under practically all scenarios glacier shrinkage will continue unabated, leading to total ice loss no later than 2026 (*SI Appendix*, Fig. S8).

Ice Core Records. The ice cores recovered in 2010 from the glaciers near Puncak Jaya, the first to bedrock, provide both an absolute constraint on ice thickness and proxy evidence to examine the role of atmospheric and sea surface warming and other potential mechanisms driving glacier loss in the region. To further understand the mechanisms driving the recently observed retreat of these glaciers, analyses were conducted on the Papua ice cores to reconstruct the past tropical Pacific climate variability. The 2 longest cores drilled on the ENF (D1, 32.13 m, and D1B, 31.25 m long; located ∼5 m apart) were analyzed for $\delta^{18}O$, δD, and concentrations of insoluble dust and major ions (17). The D2 (26.19 m) core was not analyzed as the drilling was terminated when vertical ice layers, suggesting contorted ice flow, were encountered. Basal melting was confirmed by the 0 °C temperature at the bottom of the D1 and D1B boreholes and by meltwater encountered 80 cm above the bottom of the D2 borehole. Reproducibility of the stable isotopes in both cores is illustrated (Fig. 4 *A* and *B* and *SI Appendix*, Table S5). The presence of the 1964 tritium (^3H) peak is detectable in a record of Papua precipitation at the Global Network of Isotopes in Precipitation [GNIP (24)] Jayapura station from 1957 to 1991 (*SI Appendix*, Fig. S9 *A* and *B*). This tritium peak is also recorded at 23.4-m depth in the D1 core, although its value (2.98 ± 0.42 TU) (Fig. 5*A*) is reduced due to radioactive decay over the 47 intervening years. This serves as the sole chronological marker for the timescale reconstruction. Modest precipitation seasonality in the Papua highlands (13) and post-depositional processes minimize seasonal aerosol variations in the cores (Fig. 4 *C*–*E*). Dating of the ice core records was challenging due to 1) this lack of seasonal variability, 2) the presence of only one chronological marker, and 3) melting of the glacier at both the surface and the base. However, construction of post-1964 chronologies for both cores was attempted by $\delta^{18}O$ reference matching with the NINO3 extended reconstructed sea surface temperatures [ERSST (25)]. The rationale for the matching is based on a positive, albeit weak, correlation between rainfall $\delta^{18}O$ at GNIP stations in Papua and NINO3 ERSST (*SI Appendix*, Figs. S10 and S11 and Table S6). The resulting timescales demonstrate that the ENF cores encompass at most 47 y (1964–2010 CE) in the top 23.4 m (Fig. 5*B*). The correlations between the 2 ice cores' $\delta^{18}O$ values and the NINO3 sea surface temperatures (SSTs) are statistically robust with $r = 0.58$ ($P < 0.001$) for the D1 core and $r = 0.52$ ($P < 0.001$) for the D1B core. The correlations are just slightly stronger for the 1964–1999 period with $r = 0.61$ ($P < 0.001$) for the D1 core and $r = 0.53$ ($P < 0.001$) for the D1B core. However, ablation at the surface of the glacier, which was observed during the 2010 drilling operation and subsequently documented by stake measurements (Fig. 2), may have truncated the top of the time series. The very high concentrations of soluble and insoluble aerosols in the upper ∼4 m of the ice cores (Fig. 4 *C*–*E*) illustrate the extent of this ablation, which may have accelerated in the early 21st century (∼2005) (Fig. 5 *C*–*E*). Therefore, this climate record since 1964 should not be regarded as precise at an annual resolution. Since melting is also occurring at the base of the glacier, the bottom ages of the D1 and D1B ice cores cannot be fixed, and thus timescale reconstruction for the cores was not attempted below the depth of the ^3H signal.

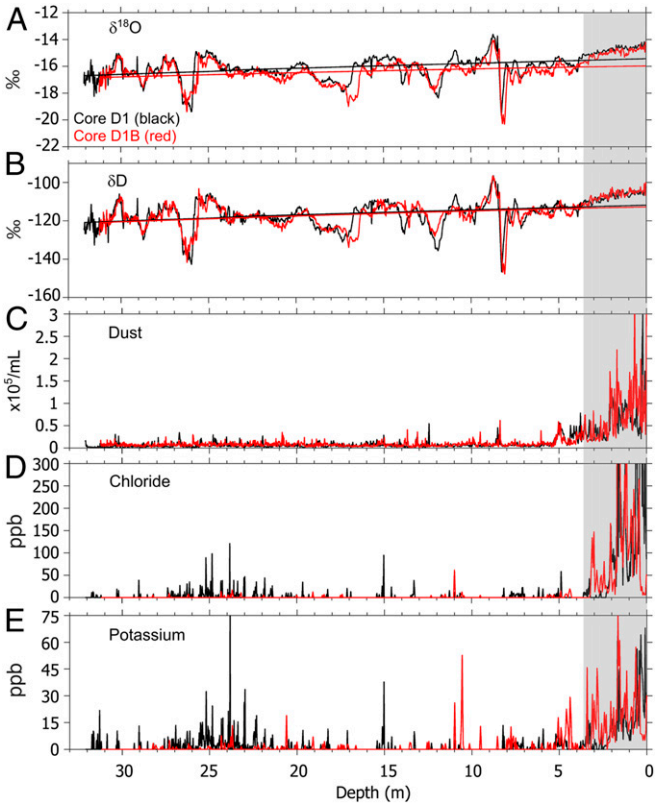

Fig. 4. Ice core records. The (*A*) $\delta^{18}O$ and (*B*) δD in the D1 (black) and D1B (red) cores show high reproducibility and positive trends toward the surface. Comparison of (*C*) mineral dust, (*D*) chloride, and (*E*) potassium concentrations among the ENF cores shows reproducibility and increased concentrations toward the top as the stable isotope variability decreases and the trend of isotopic enrichment increases (gray shading).

An independent check on the timescale is possible by comparing the core D1 tritium data (Fig. 6*A*) with the record of annual tritium in precipitation from the GNIP stations in Jayapura, Indonesia, and Madang, Papua New Guinea (*SI Appendix*, Fig. S9*A*), from 1957 to 1991 (Fig. 6*B*). Unfortunately, tritium data from these stations do not exist after 1991. However, the comparison of these records over 35 y is comparable with the ice core $\delta^{18}O$ matching with the NINO3 SST time series.

In the Tropics, precipitation $\delta^{18}O$ is negatively correlated with precipitation amount at lower altitudes and in coastal regions through the amount effect (26, 27). However, this relationship is much more complex, since stable isotopes in tropical precipitation are affected by source conditions such as SSTs, along with large-scale atmospheric circulation, transport pathways, cloud-top temperature and cloud-top pressure in convective clouds, and prevailing low-latitude upper tropospheric temperatures (10, 13, 28–33). The precipitation type also appears to influence $\delta^{18}O$, i.e., a higher proportion of convective versus stratiform precipitation results in isotopic enrichment (34). Moreover, convective precipitation is more responsive to increasing temperature than stratiform precipitation (35). The influences of coupled ocean–atmosphere processes on stable isotopes are particularly pronounced during ENSO events, which is evident in the correlation between SSTs in the equatorial Pacific and $\delta^{18}O$ in rainfall at Jayapura (*SI Appendix*, Fig. S10), which facilitated the development of the ENF ice core timescales.

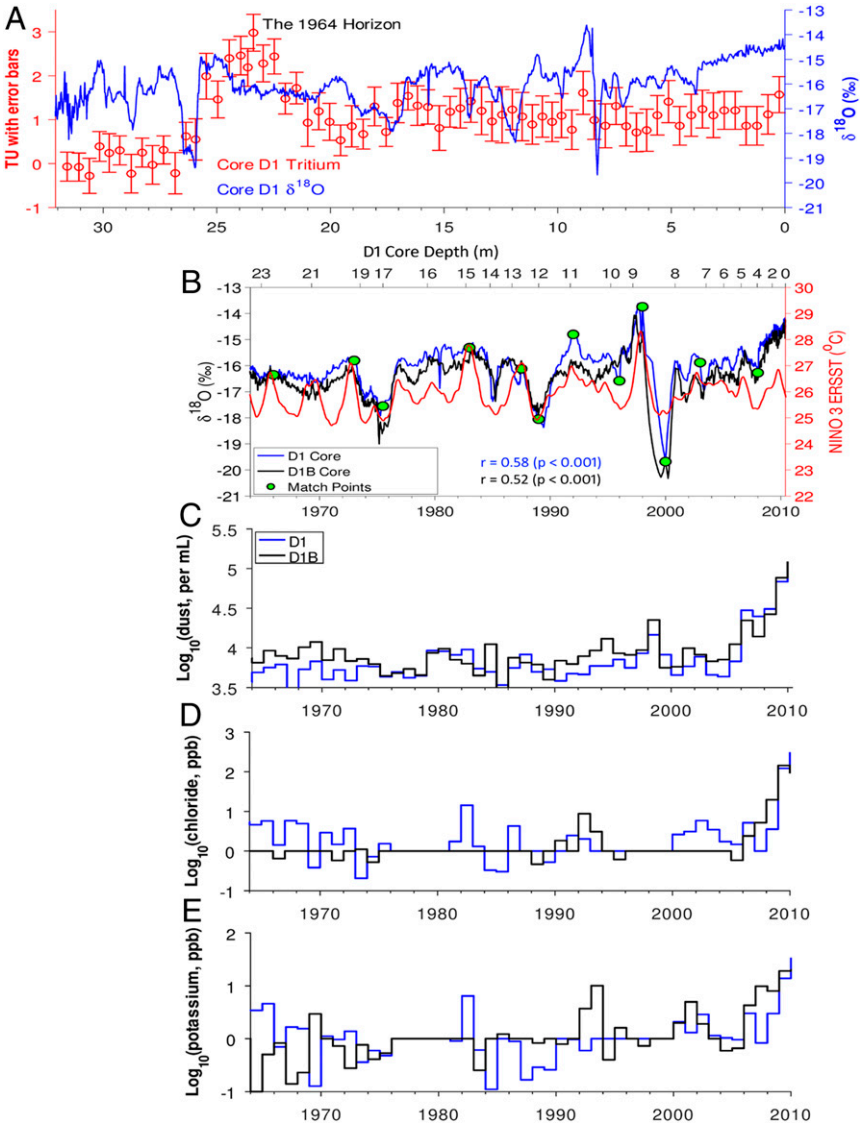

Fig. 5. Annual ice core records since 1964. (*A*) The $\delta^{18}O$ and ^{3}H data from 68 samples in D1 core (red closed circles with error bars). The 1964 horizon is marked by the ^{3}H peak (2.98 ± 0.42 TU) at 23.4-m depth. (*B*) The D1 and D1B $\delta^{18}O$ time series are compared, and 12 points in D1 (green closed circles) are paired with corresponding points in 13-mo running means of NINO3 ERSST (24) after assigning the 1964 ^{3}H peak at 23.4 m and assuming the top layer is May 2010. The correlations between the 2 ice cores' $\delta^{18}O$ values and the NINO3 SSTs are shown. (*C*) The logged values of annual averages of dust concentration (size of >0.63 μm) in the D1 and D1B cores post-1964. (*D*) As in *C*, but for chloride concentrations. (*E*) As in *C*, but for potassium concentrations.

Since the middle of the 20th century, the increasing tropical Pacific sea surface and upper level temperatures have been augmented by the effects of El Niño (36). The ENF ice core $\delta^{18}O$ records show increasing trends (*SI Appendix*, Fig. S12*A*), with an average slope of 0.018 ± 0.008‰ per year ($P < 0.03$), which reflects the trends in global and regional surface and upper level (550 mb) temperature anomalies (*SI Appendix*, Fig. S12 *B* and *C*). However, from the mid-20th century to 2010, seasonal trends in precipitation anomalies were constant (*SI Appendix*, Fig. S12*D*). This also implies that the relationship between $\delta^{18}O$ and the amount effect, which is obvious on a seasonal basis in the Tropics, is indirect on intraannual timescales. Precipitation amount and temperature are components of the complex atmospheric and oceanic processes that control the stable isotopes in the high-altitude precipitation and hence in the glacier ice.

Although the ENF ice core records contain less than a century of climate history, they serve as the only ice core-derived, high-altitude climate reconstruction from the WPWP. These ice core records not only demonstrate the deteriorating condition of these few surviving glaciers, but also provide information on the changing conditions of the atmospheric and oceanic conditions that will drive the loss of the only tropical ice fields between the Himalayas and the Andes over the next few years, especially if the loss is augmented by strong El Niños.

The glaciers near Puncak Jaya are remnants of glaciers that have existed for ~5,000 y (37, 38), and at the current rate of ice loss these glaciers will disappear in a very short time. The precise ice coverage over several years provides a reasonable determination of the variations in the rate of ice loss between El Niño and non-El Niño years.

The climate records from the ENF ice cores establish that the current glaciers have undergone significant mass loss, are melting from the surface and at the base, and have been doing so for many years, and that the rate of melting and hence the destruction of information regarding interannual climate variability is increasing. There is a strong probability that the ENF now contains fewer years than it did in 2010 as time (ice) is being removed by ablation from the bottom and the top. Along with

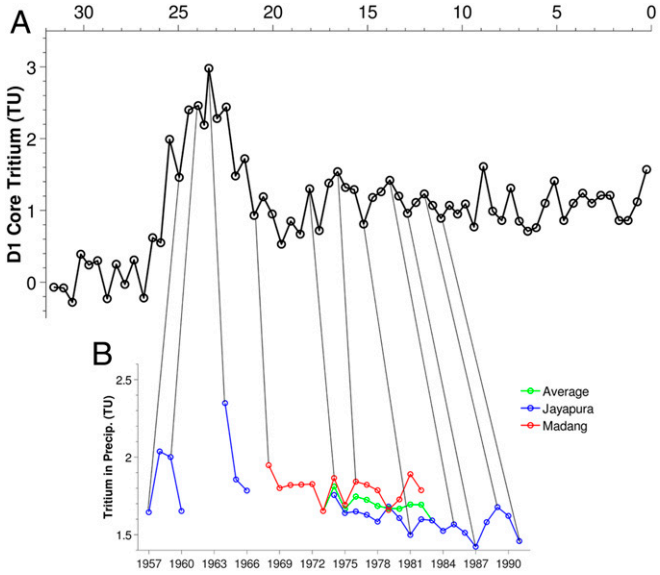

Fig. 6. Comparison of core D1 and GNIP station ^{3}H records. (*A*) The ^{3}H record from core D1 is shown in depth next to (*B*) the annual ^{3}H in precipitation collected from GNIP stations in Jayapura, Indonesia (blue curve), and Madang, Papua New Guinea (red curve), from 1957 to 1991 (*Bottom*). The green curve depicts the average ^{3}H values from the 2 stations where the records overlap (1974–1982). The thin lines connect similar features in the ice core and precipitation curves. Note that the ^{3}H concentration in precipitation collected at the stations has been calculated using the decay half-life of 12.3 y in order to show that the value of the peak in the sample collected in 1964 is compatible with that in the ice core record.

the Furtwängler Glacier on the top of Kilimanjaro (5), these cores illustrate what happens to a climate record contained in a glacier as it melts away.

Materials and Methods

Ice Surface Area and Thickness Changes. The changes in ice surface area were determined using 5 satellite images to outline and quantify the surface area of the glaciers near Puncak Jaya (Fig. 3 *B* and *C* and *SI Appendix*, Table S1). The 2002 flat image was extracted from Google Maps (stereoscopic 3D mode turned off), and all images were obtained as orthorectified products. Changes in ice thickness since June 2010 were determined by measuring the accumulation stake during subsequent visits (Fig. 2*A* and *SI Appendix*, Fig. S1 *B–D*).

Mass Balance Model and Future Projections. Volumetric changes from 2017 to 2030 were simulated using a spatially distributed model that calculates mass balance at daily time steps on each grid-cell flagged as ice or snow, according to the RGI (21). Ablation was computed from daily positive temperatures, while accumulation was calculated using temperature thresholds to determine the amount of solid precipitation falling over the glacierized area. The model was calibrated by simulating periods with available stake measurements, and identifying optimal combinations of lapse rates and degree day factors (DDFs) that reproduced the surface thinning. One thousand combinations were tested using the lapse rates shown in *SI Appendix*, Fig. S3 and published DDFs (39). Precipitation and temperature records around the study area (*SI Appendix*, Table S2) were combined to construct a relatively continuous time series for the highest elevation weather station (ALP). Simulation of future volume change was performed for the period 2017–2030 using input from 5 regional climate models over Southeast Asia [CORDEX-SEA (40)] and for 3 Coupled Model Intercomparison Project (Phase 5) experiments (historical, Representative Concentration Pathway 4.5 [RCP4.5], and RCP8.5) (*SI Appendix*, Table S4). Time series for the Puncak Jaya ice fields were obtained from bilinear interpolation of the gridded model output, and then downscaled using the cumulative distribution function-transform method (41).

Ice Core Analysis and Timescale Reconstruction. The D1 and D1B ice cores were cut into discrete samples (each ∼2 to 3 cm long), melted, and analyzed for oxygen and hydrogen isotope ratios (δ^{18}O, δD, respectively), and insoluble dust and major anion and cation concentrations. The annual means of δ^{18}O of precipitation from the GNIP station at Jayapura, Papua (1961–1991), were compared with NINO3 ERSST. The timescale reconstruction was based on identification of the 1964 peak in tritium and matching of the core D1 tritium record with tritium in precipitation from GNIP stations at Jayapura and Madang, and on δ^{18}O reference matching with NINO3 ERSST.

Detailed explanations of the methods, analysis, model simulations, and associated references are in *SI Appendix*.

ACKNOWLEDGMENTS. D.S.P., L.G.T., E.M.-T., M.E.D., P.-N.L., J.P.N., B.W.B., V.N.M., P.G., V.Z., K.R.M., U.S., and B.G.M. were supported by National Science Foundation (NSF) Grant ATM-0823586. R.D.S. was supported by NSF Grant ATM-0823617. A.F. was supported by National Fund for Scientific and Technological Development (Fondo Nacional de Desarrollo Científico y Tecnológico) Grant 11160454. D.S.P., W.H., M.N.H., and D.G. were supported by Agency for Meteorology Climatology and Geophysics (Badan Meteorologi, Klimatologi, dan Geofisika) 2009–2010 funds. Y.K. and G.S. were supported by PT Freeport Indonesia (PTFI) funds. J.F.B., V.Z., and K.R.M. are retired. We gratefully acknowledge the considerable staff and logistical support of PTFI in Indonesia. This manuscript is Byrd Polar and Climate Research Center contribution number C-1558.

1. L. G. Thompson, E. Mosley-Thompson, M. E. Davis, H. H. Brecher, Tropical glaciers, recorders and indicators of climate change, are disappearing globally. *Ann. Glaciol.* **52**, 23–34 (2011).
2. L. G. Thompson *et al.*, Annually resolved ice core records of tropical climate variability over the past ∼1800 years. *Science* **340**, 945–950 (2013).
3. F. Vimeux *et al.*, Climate variability during the last 1000 years inferred from Andean ice cores: A review of methodology and recent results. *Palaeogeogr. Palaeoclimatol. Palaeoecol.* **281**, 229–241 (2009).
4. R. G. Taylor *et al.*, Recent glacial recession in the Rwenzori Mountains of East Africa due to rising air temperature. *Geophys. Res. Lett.* **33**, L10402 (2006).
5. L. G. Thompson *et al.*, Kilimanjaro ice core records: Evidence of Holocene climate change in tropical Africa. *Science* **298**, 589–593 (2002).
6. A. G. Klein, J. L. Kincaid, Retreat of glaciers on Puncak Jaya, Irian Jaya, determined from 2000 and 2002 IKONOS satellite images. *J. Glaciol.* **52**, 65–79 (2006).
7. M. L. Prentice, S. Glidden, *Altered Ecologies: Fire, Climate and Human Influence on Terrestrial Landscapes*, S. Haberle, J. Stevenson, M. Prebble, Eds. (ANU Press, Canberra, ACT, Australia, 2010), pp. 457–471.
8. P. Wagnon, P. Ribstein, B. Francou, J. E. Sicart, Anomalous heat and mass budget of glacier Zongo, Bolivia, during the 1997/98 El Niño year. *J. Glaciol.* **47**, 21–28 (2001).
9. B. Francou, M. Vuille, V. Favier, B. Cáceres, New evidence for an ENSO impact on low-latitude glaciers: Antizana 15, Andes of Ecuador, 0 28′S. *J. Geophys. Res.* **109**, D18106 (2004).
10. L. G. Thompson *et al.*, Impacts of recent warming and the 2015/16 El Niño on tropical Peruvian ice fields. *J. Geophys. Res. Atmos.* **122**, 12688–12701 (2017).
11. G. Chen, H. Qin, Strong ocean-atmosphere interactions during a short-term hot event over the Western Pacific Warm Pool in response to El Niño. *J. Clim.* **29**, 3841–3865 (2016).
12. M. L. Prentice, G. S. Hope, *The Ecology of Papua: Part One*, A. J. Marshall, B. M. Beehler, Eds. (Periplus Editions, Singapore, 2007), pp. 177–195.
13. D. S. Permana, L. G. Thompson, G. Setyadi, Tropical West Pacific moisture dynamics and climate controls on rainfall isotopic ratios in southern Papua, Indonesia. *J. Geophys. Res. Atmos.* **121**, 2222–2245 (2016).
14. S. G. Haberle, G. S. Hope, S. van der Kaars, Biomass burning in Indonesia and Papua New Guinea: Natural and human induced fire events in the fossil record. *Palaeogeogr. Palaeoclimatol. Palaeoecol.* **171**, 259–268 (2001).
15. M. Zemp *et al.*, Historically unprecedented global glacier decline in the early 21st century. *J. Glaciol.* **61**, 745–762 (2015).
16. A. Rabatel *et al.*, Current state of glaciers in the tropical Andes: A multi-century perspective on glacier evolution and climate change. *Cryosphere* **7**, 81–102 (2013).
17. D. S. Permana, "Reconstruction of tropical Pacific climate variability from Papua ice cores, Indonesia," PhD thesis, Ohio State University, Columbus, OH (2015).
18. J. A. Peterson, L. F. Peterson, Ice retreat from the neoglacial maxima in the Puncak Jayakesuma area, Republic of Indonesia. *Z. Gletsch. kd. Glazialgeol.* **30**, 1–9 (1994).
19. Q. van Ufford, P. Sedgwick, Recession of the equatorial Puncak Jaya glaciers (∼1825 to 1995), Irian Jaya (Western New Guinea), Indonesia. *Z. Gletsch. kd. Glazialgeol.* **34**, 131–140 (1998).
20. J. L. Kincaid, "An assessment of regional climate trends and changes to the Mt. Jaya glaciers of Irian Jaya," master's thesis, Texas A&M University, College Station, TX (2007).
21. W. T. Pfeffer *et al.*, The Randolph glacier inventory: A globally complete inventory of glaciers. *J. Glaciol.* **60**, 537–552 (2014).
22. D. B. Bahr, M. F. Meier, S. D. Peckham, The physical basis of glacier volume-area scaling. *J. Geophys. Res. Solid Earth* **102**, 20355–20362 (1997).
23. I. Gärtner-Roer *et al.*, A database of worldwide glacier thickness observations. *Global Planet. Change* **122**, 330–344 (2014).

24. IAEA/WMO, Global network of isotopes in precipitation. The GNIP database (2018). https://www.iaea.org/services/networks/gnip. Accessed 15 June 2018.
25. B. Huang *et al*., Extended Reconstructed Sea Surface Temperature, Version 4 (ERSST. V4). Part I: Upgrades and intercomparisons. *J. Clim.* **28**, 911–930 (2015).
26. W. Dansgaard, Stable isotopes in precipitation. *Tellus* **16**, 436–468 (1964).
27. K. Rozanski, L. Araguás-Araguás, R. Gonfiantini, *Climate Change in Continental Isotopic Records*, P. K. Swart, K. C. Lohmann, J. McKenzie, S. Savin, Eds. (AGU, Washington, DC, 1993), pp. 1–36.
28. R. S. Bradley, M. Vuille, D. R. Hardy, L. G. Thompson, Low latitude ice cores record Pacific sea surface temperatures. *Geophys. Res. Lett.* **30**, 1174 (2003).
29. Z. Cai, L. Tian, Atmospheric controls on seasonal and interannual variations in the precipitation isotope in the East Asian Monsoon region. *J. Clim.* **29**, 1339–1352 (2016).
30. K. E. Samuels-Crow *et al*., Upwind convective influences on the isotopic composition of atmospheric water vapor over the tropical Andes. *J. Geophys. Res. Atmos.* **119**, 7051–7063 (2014).
31. M. A. Scholl, J. B. Shanley, J. P. Zegarra, T. B. Coplen, The stable isotope amount effect: New insights from NEXRAD echo tops, Luquillo Mountains, Puerto Rico. *Water Resour. Res.* **45**, W12407 (2009).
32. M. Vuille *et al*., Modeling δ^{18}O in precipitation over the tropical Americas: 2. Simulation of the stable isotope signal in Andean cores. *J. Geophys. Res.* **108**, 4175 (2003).
33. J. V. Hurley, M. Vuille, D. R. Hardy, S. J. Burns, L. G. Thompson, Cold air incursions, δ^{18}O variability, and monsoon dynamics associated with snow days at Quelccaya Ice Cap, Peru. *J. Geophys. Res.* **120**, 7467–7487 (2015).
34. P. K. Aggarwal *et al*., Proportions of convective and stratiform precipitation revealed in water isotope ratios. *Nat. Geosci.* **9**, 624–629 (2016).
35. P. Berg, C. Moseley, J. O. Haerter, Strong increase in convective precipitation in response to higher temperatures. *Nat. Geosci.* **6**, 181–185 (2013).
36. R. Seager *et al*., Strengthening tropical Pacific zonal sea surface temperature gradient consistent with rising greenhouse gases. *Nat. Clim. Chang.* **9**, 517–522 (2019).
37. G. S. Hope, J. A. Peterson, Glaciation and vegetation in the high New Guinea Mountains. *Bull. R. Soc. N. Z.* **13**, 155–162 (1975).
38. E. Loffler, *Biogeography and Ecology of New Guinea* (Monographiae Biologicae, Junk, The Hague, The Netherlands, 1982), vol. 42, pp. 39–55.
39. R. Hock, Glacier melt: A review of processes and their modelling. *Prog. Phys. Geogr: Earth and Environment* **29**, 362–391 (2005).
40. J. X. Chung, J. Liew, T. Fredolin, A. F. Jamaluddin, Performances of BATS and CLM land-surface schemes in RegCM4 in simulating precipitation over CORDEX Southeast Asia domain. *Int. J. Climatol.* **38**, 794–810 (2017).
41. P. A. Michelangeli, M. Vrac, H. Loukos, Probabilistic downscaling approaches: Application to wind cumulative distribution functions. *Geophys. Res. Lett.* **36**, 2–7 (2009).